2011

Closed-shell to split-shell stability of isovalent clusters

Victor M. Medel
Virginia Commonwealth University

J. Ulises Reveles
Virginia Commonwealth University

A. C. Reber
Virginia Commonwealth University

Shiv N. Khanna
Virginia Commonwealth University, snkhanna@vcu.edu

A. W. Castleman Jr.
Pennsylvania State University

Medel, V.M., Reveles, J.U., Reber, A.C., et al. Closed-shell to split-shell stability of isovalent clusters. Physical Review B, 84, 075435 (2011).

Closed-shell to split-shell stability of isovalent clusters

Victor M. Medel, J. Ulises Reveles, A. C. Reber, and Shiv N. Khanna*
Department of Physics, Virginia Commonwealth University, Richmond, Virginia 23284, USA

A. W. Castleman Jr.
Departments of Chemistry and Physics, Penn State University, State College, Pennsylvania 16802, USA
(Received 4 March 2011; revised manuscript received 11 May 2011; published 8 August 2011)

Metallic clusters containing 2, 8, 18, and 20 electrons are now known to exhibit enhanced stability that can be reconciled because of filled 1S, 1P, 1D, and 2S electronic shells within a simplified confined nearly free electron (NFE) gas. Here, we present first-principles studies on three isovalent clusters, i.e., $ZnMg_8$, $CuMg_8^-$, and $AuMg_8^-$, each with 18 valence electrons. All the clusters exhibit local energetic stability but with differing origins. Although the stability of $ZnMg_8$ can be reconciled within the conventional confined NFE picture with filled $1S^2$, $1P^6$, and $1D^{10}$ shells, $CuMg_8^-$ and $AuMg_8^-$ are shown to be stable despite the unfilled D-shell. Their stability can be understood as a crystal field–like splitting of the otherwise degenerate D-shell because of internal electric fields of the positive ion cores that lead to a filled $1S^2$, $1P^6$, $1D^8$, $2S^2$ sequence separated by unfilled D^2 states that form a large gap. We also examine the progression toward the metallic character in $ZnMg_n$ clusters, because isolated Mg and Zn atoms have filled valence $4s^2$ and $3s^2$ atomic states. As Mg atoms are added to a Zn atom, the excited atomic p-states in the Mg atoms hybridize rapidly with Zn and Mg s-states to promote a metallic character that evolves more rapidly than in pure Mg_n clusters.

DOI: 10.1103/PhysRevB.84.075435 PACS number(s): 36.40.Cg

I. INTRODUCTION

The quantum confinement of electrons in spherical clusters leads to bunching of electronic levels into shells much in the same way as in atoms.[1] In addition, the electronic orbitals in these shells, although generally spread over multiple atoms, have shapes similar to atomic orbitals.[2–4] These analogies have given rise to the concept of superatoms, i.e., selected clusters with stable chemical valence mimicking atoms in the periodic table.[4] A simple model incorporating these features is the Jellium model, where the electrons respond to a positive uniform background obtained by smearing the charge of ionic cores.[2,3] Over the past two dozen years, this model has offered a generalized understanding of the cluster behaviors in a range of metallic clusters.[1–20] In particular, clusters with filled electronic shells and large gaps between the highest occupied molecular orbital (HOMO) and the lowest unoccupied molecular orbital (LUMO) are found to exhibit enhanced stability and reduced reactivity. These account for the magic numbers at electron counts $n^* = 2$, 8, 18, 20, 34, 40, 58, 68, 70, . . ., corresponding to the filled 1S, 1P, 1D, 2S, 1F, 2P, 1G, 2D, 3S, . . . shells, respectively, observed in alkali and other metal clusters, as well as the observed inertness of Al_{13}^- (throughout this paper, the atomic orbitals are marked by lowercase letters, whereas the orbitals in clusters are denoted by uppercase letters).[21–23]

The degenerate electronic states in atoms are known to undergo splitting as the spherical potential is modified.[22,24,25] A simple example is the crystal field splitting of the d-states of transition metal ions in the electrostatic fields of surrounding charges. Depending on the charge and the symmetry of the surrounding ions, the d-states can be split into various groups separated by large energies. In particular, a square antiprism arrangement splits the d-states into three groups consisting of (1) d_{xz}, d_{yz}, (2) $d_{x^2-y^2}$, d_{xy}, and (3) d_{z^2} states. In a recent work, we proposed that the splitting of supershells can lead to stable clusters with filled subshells.[13] Our work focused on the reactivity of $CuAl_n^-$ clusters with oxygen, where the experiments showed that $CuAl_{22}^-$ was a highly stable species. Accompanying theoretical calculations showed that the etching resistance of $CuAl_{22}^-$ could be explained by an unusually large splitting of the $2D^{10}$ subshell that occurs because of a geometric distortion of the cluster that amounts to a compression along the z-axis.

In this paper, we present an interesting scenario involving three stable clusters, i.e., $ZnMg_8$, $CuMg_8^-$, and $AuMg_8^-$, each containing 18 valence electrons. A shell closure at 18 electrons occurs in the Jellium picture for a filling of $1S^2$ $1P^6$ $1D^{10}$ supershells, and this could account for their stability. On the other hand, a crystal field splitting similar to those in atoms could also lead to a shell closure that has a $1S^2$ $1P^6$ $1D^8$ $2S^2$ shell structure with excited unfilled $1D^2$ levels. In this work, we use first-principles methods to investigate the electronic states in these clusters and show how the level structure can be qualitatively rationalized within this simple Jellium model by using ideas of crystal field splitting. Our studies based on first-principles electronic structure calculations show how either one or the other supershell sequence evolves as a function of size from Cu to Au, and as a function of charge and valence in $ZnMg_8$, to stabilize the cluster. We also analyze the evolution of geometry and electronic structure of $ZnMg_n$ clusters containing up to 12 Mg atoms from another perspective. A Mg atom has a closed $3s^2$ valence state with unfilled 3p excited states. Mg_2 is a weakly bound van der Waals dimer, whereas bulk Mg is a metal. Previous studies on isolated Mg_n clusters have shown that a transition toward metallic character evolves as more Mg atoms are brought together to form larger units.[26] This transition is linked to the mixing of the valence s-states with the excited p-states. The mixing evolves rapidly with size, and a cluster containing 6 Mg atoms already has 23% of the p-character. Like Mg, Zn

also has a closed-shell $4s^2$ state followed by an excited 4p level. We wanted to examine how the presence of Zn would affect the mixing between the s- and the p-states in the composite clusters.

Section II presents the details of the theoretical method, and Sec. III presents the theoretical findings and a discussion of the results. Sec. IV concludes our findings.

II. THEORETICAL METHODS

The ground state geometries, one-electron states, and molecular orbitals of $ZnMg_n$ clusters ($n = 1$–12), $CuMg_8^-$, and $AuMg_8^-$ were calculated using a linear combination of Gaussian orbitals and a molecular orbital approach within a density functional theory formalism. Calculations were performed using the deMon2k code[27] with a gradient-corrected Perdew-Burke-Ernzerhof functional.[28] Basis sets consisted of a double-ζ valence plus polarization type of (6321/411/1*) with 4s, 3p, and 1d Gaussians for Mg and (63321/531/41*) with 5s, 3p, and 2d Gaussians for Cu and Zn.[29] For Au, we used a relativistic effective core potential with 19 valence electrons with a RECP19ISD valence basis set (2111111/411/2111) of 7s, 3p, and 4d Gaussians.[30] The electronic orbitals of the clusters were assigned subshell distinctions based on the symmetry group of the molecular orbitals whenever possible and through inspection of the nodes in the calculated wave functions. The preceding analysis allowed a fairly clear assignment of the orbitals in all undistorted cases, allowing in turn a correspondence to the orbitals in the nearly free electron (NFE) Jellium model. For each size, 20–50 trial geometries were fully optimized without constraints in delocalized internal coordinates,[31] starting with known geometries for other clusters and those obtained using a genetic algorithm method.[32]

III. RESULTS

Fig. 1 shows the ground state geometry of $ZnMg_n$ clusters. Like pure Mg_n clusters, the ground state structures are all compact. $ZnMg_5$ resembles a fragment of the bulk hexagonal Mg, distorted by the Zn atom. $ZnMg_7$ is the smallest cluster to contain an interior Zn atom. $ZnMg_{12}$, with an endohedral Zn atom, has a C_{2v} symmetry with a structure dominated by triangular faces. A structure in which a Zn atom was forced to occupy an outside site was substantially higher in energy. The evolutions in geometry are accompanied by changes in bond lengths. The Mg-Mg bond length decreases from 3.3 Å in $ZnMg_2$ to 3.1 Å in $ZnMg_{12}$. This is compared to the experimental Mg-Mg bond lengths of 3.89 Å in Mg_2[33] and 3.20 Å in bulk Mg.[34] The Zn-Mg bond length also decreases from 3.3 Å in ZnMg to an average of 2.8 Å in $ZnMg_{12}$. Previous studies on pure Mg_n clusters have observed similar shortening of bond length with increasing size. The decreasing bond length is accompanied by an increase in binding. Fig. 2(a) shows the atomization energy per atom (AE/atom) as a function of size calculated using the equation

$$\mathrm{AE/atom} = (\mathrm{E(Zn)} + n\mathrm{E(Mg)} - \mathrm{E(ZnMg_n)}/(n+1)).$$

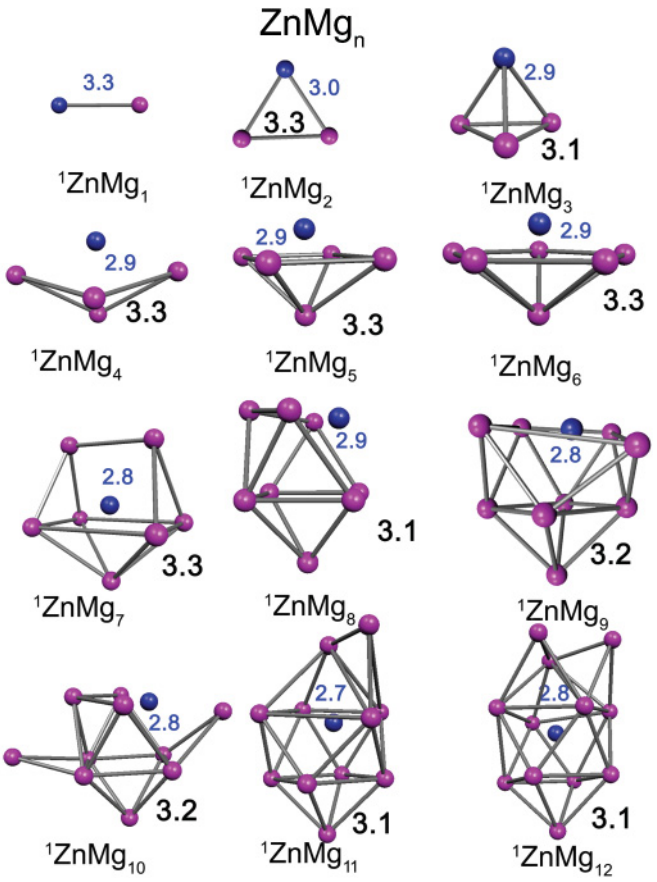

FIG. 1. (Color online) Ground state geometries of $ZnMg_n$ ($n = 1$–12) clusters. The superscripts indicate the spin multiplicity. The darker (blue) circles represent the Zn atoms, and the lighter (pink) ones represent the Mg atoms. The lighter (blue) numbers are the average distances from the Zn to the nearest Mg atoms. The dark (black) numbers are the average distances between nearest Mg atoms. All distances are in angstroms.

Here, E(Zn), E(Mg), and E($ZnMg_n$) are the total energies of a Zn atom, Mg atom, and $ZnMg_n$ cluster, respectively. The AE/atom is only 0.065 eV/atom in ZnMg, typical of a weak van der Waals type interaction, although it attains a value of 0.65 eV/atom in $ZnMg_9$, typical of metallic bonding. The 10-fold increase in binding from a molecule to a cluster of only 10 atoms is thus indicative of a change in the bonding character. To further probe this change and to look for any especially stable species, we monitored the increase in binding energy as successive Mg atoms were added to a Zn atom. The incremental binding energy (IBE) for a $ZnMg_n$ cluster was calculated using the expression

$$\mathrm{IBE} = \mathrm{E(Mg)} + \mathrm{E(ZnMg_{n-1})} - \mathrm{E(ZnMg_n)}.$$

Here, E(Mg), E($ZnMg_{n-1}$), and E($ZnMg_n$) are the total energies of a Mg atom, $ZnMg_{n-1}$ cluster, and $ZnMg_n$ cluster, respectively. The basis set superposition error for the IBE was calculated using the counterpoise method of Boys and Bernardi[35] and found to be on the order of 0.02 eV. Being a negligible contribution, it was not included in the IBEs.

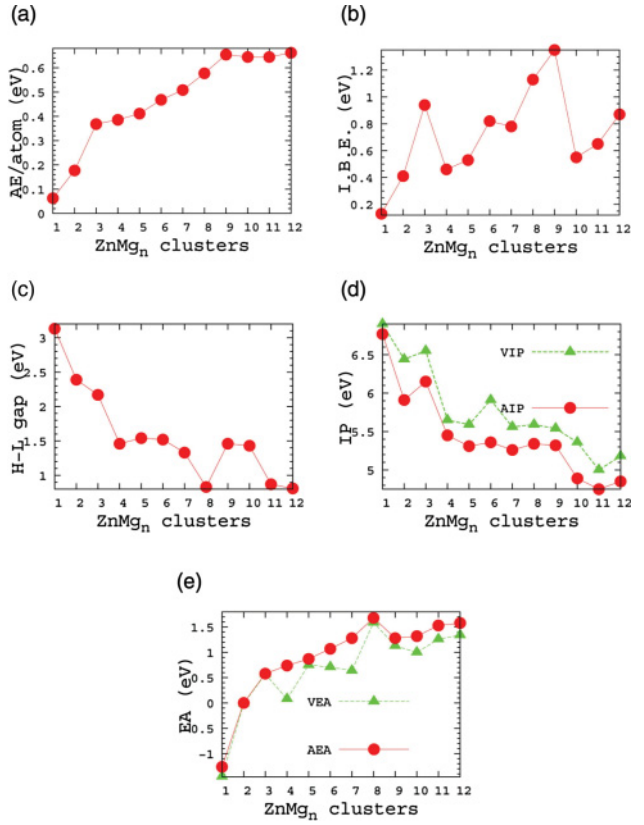

FIG. 2. (Color online) (a)Variation of the atomization energy, (b) IBE, (c) H-L gap, (d) VIP and AIP, and (e) VEA and AEA of $ZnMg_n$ clusters as a function of the *n* number of Mg atoms. The energies are in electron volts.

The calculated IBEs are shown in Fig. 2(b). Starting from ZnMg, the addition of Mg atoms increases the IBE, and $ZnMg_3$ already has an IBE of 0.9 eV. Because the cluster has 8 valence electrons, 2 from Zn ($4s^2$) and 6 from the 3 Mg atoms ($3s^2$), we could assign its enhanced stability to the shell closure at 8 electrons in a Jellium model ($1S^2$, $1P^6$). The other two clusters that have a high IBE are $ZnMg_8$ and $ZnMg_9$, with an IBE of 1.13 and 1.35 eV, respectively, compared to an AE/atom of 1.51 eV in bulk Mg.[36] These clusters have 18 and 20 valence electrons, and the enhanced stability matches with a shell closure of 18 and 20 valence electrons, respectively. These results suggest that the addition of Mg atom starting from ZnMg leads to evolution of the nature of bonding toward a NFE character. In addition to a larger IBE, we examined the gap between the HOMO and LUMO (the H-L gap). Fig. 2(c) shows the variation of the H-L gap in $ZnMg_n$ clusters, and all the clusters have gaps exceeding 0.8 eV. We also calculated other electronic features. Fig. 2(d) shows the vertical ionization potential (VIP) and adiabatic ionization potential (AIP) of the clusters, corresponding to the energy required to remove an electron from the neutral cluster to generate a cation with unrelaxed and relaxed cation geometry, respectively. The electron affinity (EA) of the clusters was calculated as the gain in energy as an electron is added to the neutral species. Both the vertical electron affinity (VEA) and the adiabatic electron affinity (AEA) were calculated by taking the energy of the unrelaxed and relaxed anions, respectively, and the trend is shown in Fig. 2(e). The IPs show a decreasing trend with size, whereas the EAs increase starting from the smallest size. Typical shell filling in a confined NFE gas has a high IBE, along with peaks in the IP and a dip in the EA. Although the IBE shows peak behavior for $ZnMg_8$ and $ZnMg_9$, the other signatures are not visible. We believe that the progressions in bonding characteristics are overriding the shell effects. In addition, Fig. 2(b) and (c) shows that the shell closure at 20 e^- ($ZnMg_9$) is really marked, because the IBE shows a sharp drop after $ZnMg_9$ and the H-L gap shows local maxima. In this work, however, we are focusing only on 18 e^- clusters.

TABLE I. Contributions in percentage coming from s- and p-states for each atomic type.

Influence of atomic orbitals in the $ZnMg_n$ clusters				
# Mg	% s Zn	% p Zn	% s Mg	% p Mg
1	47.5	2.1	48.0	2.4
2	28.8	4.0	58.1	9.1
3	18.8	5.6	56.9	18.7
4	14.0	5.3	62.1	18.6
5	10.7	5.2	64.6	19.4
6	8.9	4.3	62.5	24.3
7	6.6	5.0	63.2	25.3
8	6.9	3.5	56.5	33.1
9	5.4	4.0	55.6	34.9
10	5.0	3.6	57.8	33.7
11	4.0	3.7	57.5	34.7
12	3.6	3.5	57.1	35.7

The reason for these variations is that although ZnMg is a weakly bound molecule, the addition of Mg atoms promotes the transition from a van der Waals to a NFE character. Such a transition of bonding character has previously been investigated in Be_n,[37–39] Mg_n,[26] and Hg_n[40] clusters. These clusters undergo a transition toward the metallic (NFE) behavior via mixing between the occupied s- and the unfilled p-states in the atom. To examine the prospect of a similar transition in $ZnMg_n$ clusters, we projected the molecular orbital charge densities into contributions from the Zn and Mg sites. These contributions were further analyzed into the percentage coming from s- and p-states for each atomic type. The results are given in Table I. The p-component that has a contribution from Mg p- and Zn p-states grows rapidly with size. For example, $ZnMg_3$ already has an almost 25% p-character. This is much faster than in pure Mg clusters, where previous studies indicate that a cluster containing four atoms has a less than 15% p-component.[26] The rapid increase in p-character is linked to the heteroatomic nature of the cluster, where the s-states of Zn are closer to the unfilled p-states of Mg and strongly hybridize with them. Although the percentage contribution from s-electrons of Zn rapidly decreases with increasing size because of the proportional increase in the number of Mg sites, the p-component initially increases and then shows a mild decrease. Additional p-character is also derived from the Mg-Mg interactions that promote s-electrons to p-states as the size is increased.

The progression toward a NFE character is clearly seen in the nature of the electronic orbitals. Fig. 3 shows the one-electron levels, as well as the associated electronic orbitals

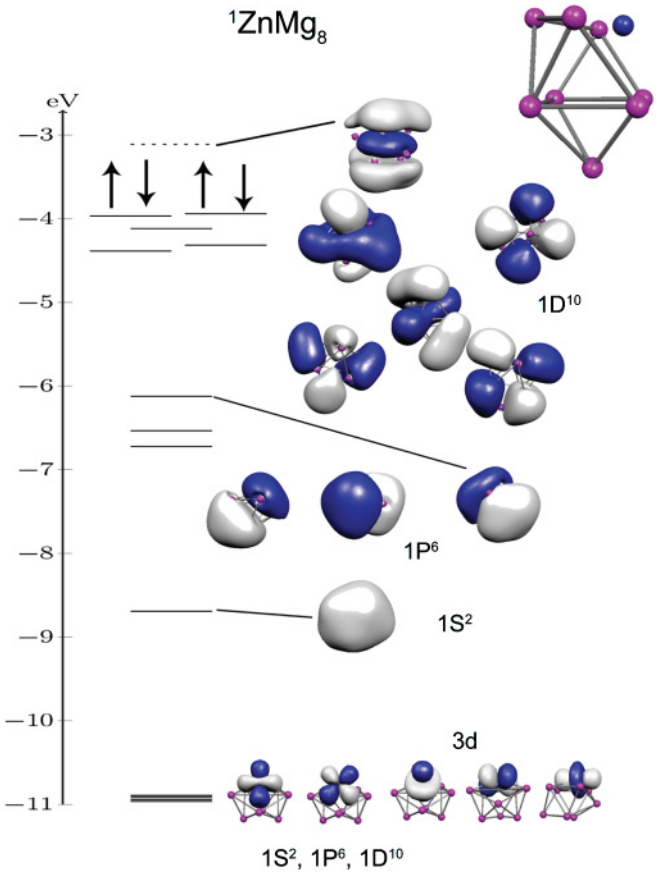

FIG. 3. (Color) One-electron energy levels and orbital wavefunction isosurfaces (isoval = 0.01 a.u.) of the $^1ZnMg_8$ cluster. The majority and minority levels for the ground state are shown. The continuous lines correspond to the filled levels, whereas the dotted line corresponds to the LUMO. For each level, the angular momentum is marked. The optimized geometry is also shown.

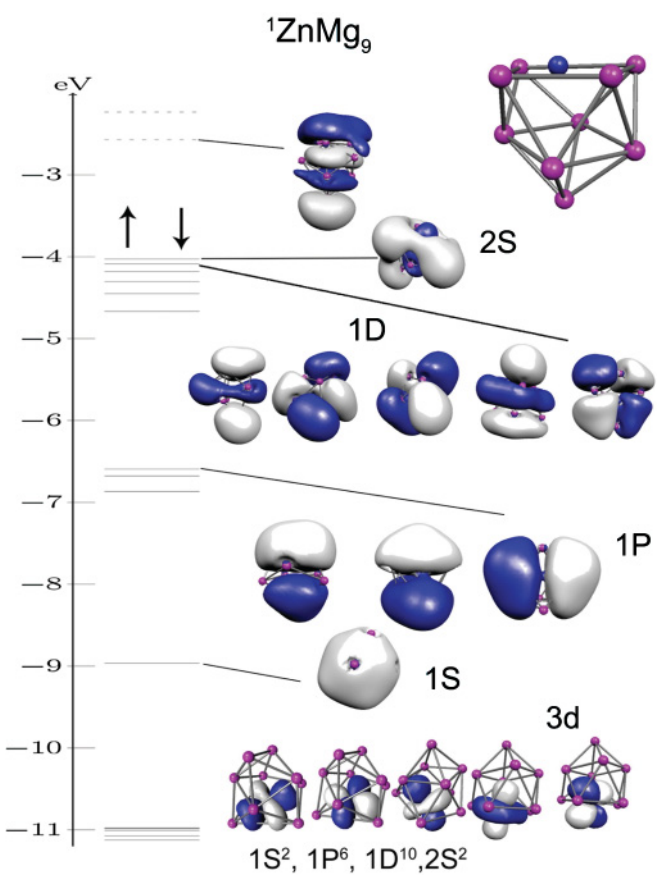

FIG. 4. (Color) One-electron energy levels and orbital wavefunction isosurfaces (isoval = 0.01 a.u.) of the $^1ZnMg_9$ cluster. The majority and minority levels for the ground state are shown. The continuous lines correspond to the filled levels, whereas the dotted line corresponds to the LUMO. For each level, the angular momentum is marked. The optimized geometry is also shown.

in the approximately spherical $ZnMg_8$ cluster. An isolated Zn atom has a filled 3d atomic core shell that forms the lowest electronic state in Fig. 3. Because the core d-states are fairly deep, they retain their atomic character and become the 3d eigenstates of the composite Hamiltonian. The remaining valence spectrum is then marked by states that can be roughly classified by the shape of the cluster orbitals. Starting around −9 eV is a spherical orbital fairly spread over the cluster that can be classified as a 1S orbital. Following this, three delocalized orbitals resembling p-states can be labeled P_x, P_y, and P_z orbitals. Above these is a group of five orbitals whose shapes closely resemble those of d-orbitals. These form the 1D-shell, which is followed by an unoccupied state separated from the filled orbitals by 0.83 eV. The unfilled state is fairly symmetric and is labeled the 2S state. The orbital shapes therefore conform to a confined NFE gas shell structure and reiterate the evolution toward metallic character. This is further seen in the electronic orbitals in $ZnMg_9$ (Fig. 4), where the 2S state becomes filled by the extra two electrons from the Mg atom, thus having filled 1S, 1P, 1D, and 2S shells. We believe that the typical pointers of large H-L gap, local peaks in IP, and minima in EA seen in metal clusters are masked by the evolution in bonding character.

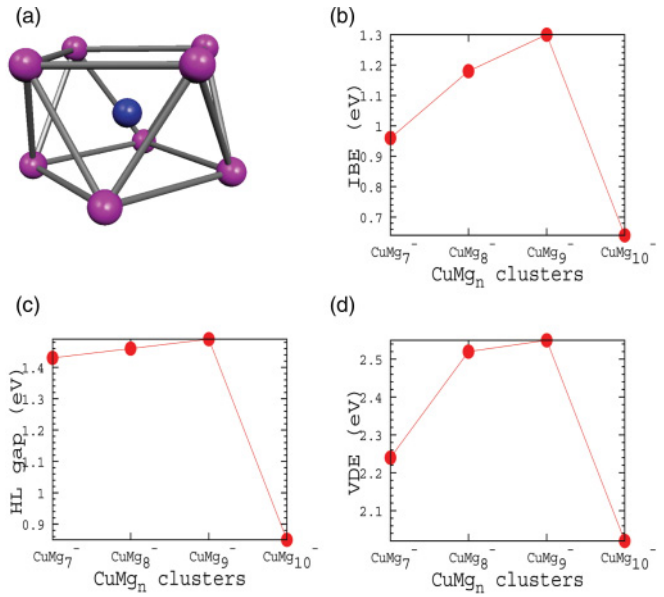

FIG. 5. (Color online) (a) $CuMg_8^-$ ground state geometry, (b) variation of the IBE, (c) H-L gap, and (d) VDE of $CuMg_n^-$ clusters as a function of the *n* number of Mg atoms. The energies are in electron volts.

Because the mixing between Mg and Zn accelerated the increase of p-character compared to pure clusters, we began to ask whether other 18 electron clusters would show a similar shell structure—in particular, whether other 18-electron systems composed of heteroatomic metal atoms would have the electronic level ordering seen in $ZnMg_8$. From an experimental point of view, the development of negative ion photo-detachment spectra and velocity map imaging techniques provided excellent experimental probes to the electronic structure and orbitals of anionic clusters, and we sought to consider anionic systems that might exhibit similar features.[41–43] Two clusters, $CuMg_8^-$ and $AuMg_8^-$, were investigated. Cu is a smaller atom, whereas Au is bigger. We wanted to see whether size had an effect on level ordering. Our structural optimization search indicated that the ground state for $CuMg_8^-$ was a different structure. The Cu atom occupied an interior site with a Mg core in a square antiprism arrangement with an oblate shape, as shown in Fig. 5(a). To examine the stability of the cluster, we calculated the IBE, the H-L gap, and the vertical detachment energy (VDE) in $CuMg_n^-$ clusters containing 7–10 Mg atoms. The results are shown in Fig. 5(b)–5(d). $CuMg_8^-$ has a large IBE (1.18 eV), a large H-L gap (1.46 eV), and a high adiabatic VDE (2.52 eV), indicative of its overall stability. The large H-L gap of $CuMg_8^-$ (1.46 eV) compared to that in $ZnMg_8$ (0.83 eV) is intriguing.

An analysis of the electronic orbitals indicated that the origin of the H-L gap is closely related to the change in shape. The ground state of $CuMg_8^-$ is a square antiprism that can be regarded as an oblate distortion of the more spherical $ZnMg_8$ cluster. As we have previously shown, such a distortion can substantially split the d_z^2 level from the d-states. To demonstrate this, we show in Fig. 6 the one-electron eigenvalues and associated molecular orbitals for $CuMg_8^-$. The cluster does not have a filled D-shell. The shell ordering corresponds to $1S^2$, $3d^{10}$, $2S^2$, and $1D^8$ filled levels with an unfilled $1D_z^2$ state that is almost 1.46 eV higher than the filled D-states. This large splitting leads to a highly stable species. The oblate distortion even leads to oblate shapes for the S-states. Finer grouping of levels may be qualitatively rationalized by considering the position of ionic cores. As mentioned in the introduction, an atomic d-state is known to split into (1) d_{xz}, d_{yz}, (2) $d_x^2-_y^2$, d_{xy}, and (3) d_z^2 groups in the presence of a square antiprism arrangement of positive charges. Here, the ionic cores lead to a similar splitting of the D-supershell into groups of 2, 2, and 1 state, with enhanced splitting between the d_{xz}, d_{yz}, and d_z^2. The main effect, however, is that the oblate distortion

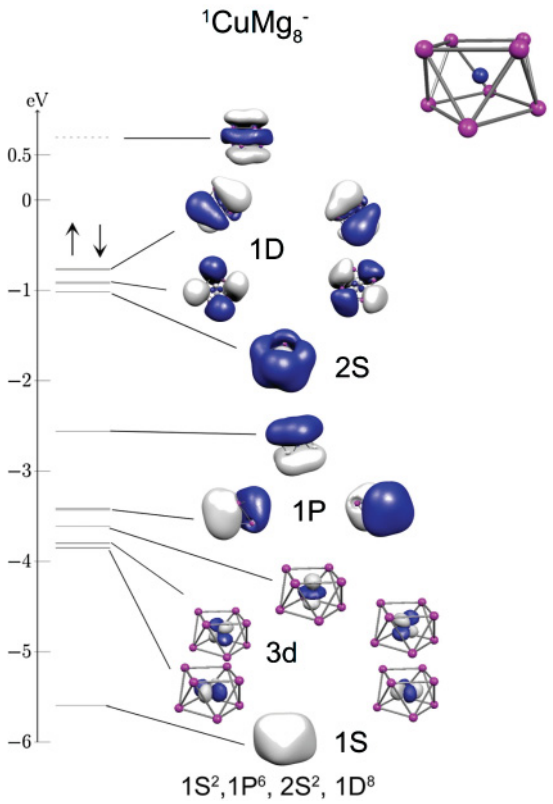

FIG. 6. (Color) One-electron energy levels and orbital wavefunction isosurfaces (isoval = 0.01 a.u.) of the $^1CuMg_8^-$ cluster. The majority and minority levels for the ground state are shown. The continuous lines correspond to the filled levels, whereas the dotted line corresponds to the LUMO. For each level, the angular momentum is marked. The optimized geometry is also shown.

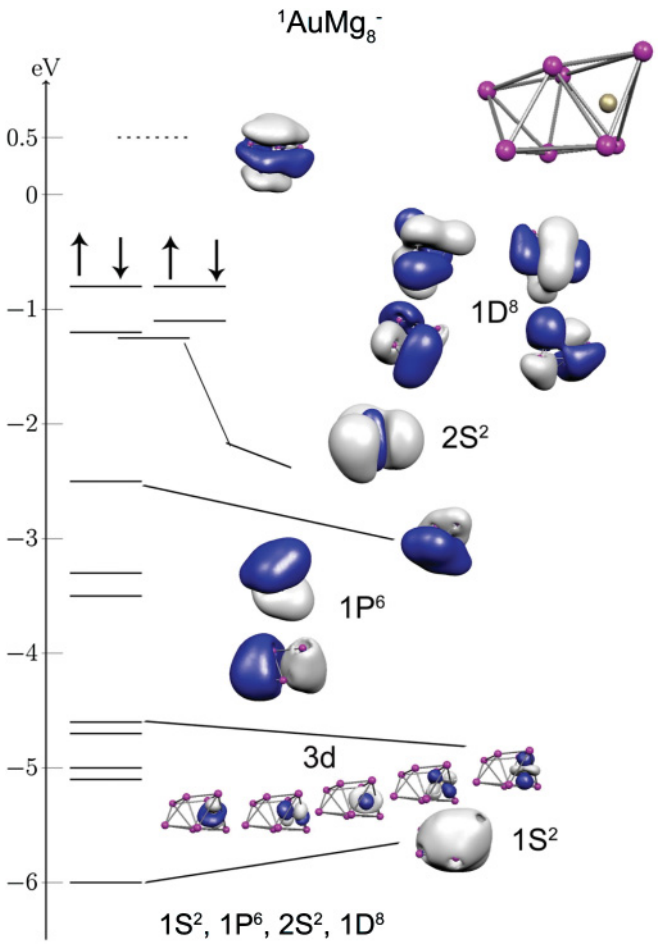

FIG. 7. (Color) One-electron energy levels and orbital wavefunction isosurfaces (isoval = 0.01 a.u.) of the $^1AuMg_8^-$ cluster. The majority and minority levels for the ground state are shown. The continuous lines correspond to the filled levels, whereas the dotted line corresponds to the LUMO. For each level, the angular momentum is marked. The optimized geometry is also shown.

destabilizes wave functions with nodes along the z-axis. What is remarkable is that the splitting can be reduced by changing the shape of the cluster. For example, our studies show that the addition of a Mg atom to generate $CuMg_9^-$ leads to a more spherical distribution of charges. Analysis of the electronic states shows that for $CuMg_9^-$ the five D-states now group into a closer bunch as expected for a spherical Jellium.

We further proceeded to demonstrate that the crystal field splitting could be altered by changing the oblateness. This can be accomplished by replacing Cu by a larger atom that would deform the cluster. To this end, we examined the ground state geometry and associated electronic structure of an $AuMg_8^-$ cluster. The ground state structure is a distorted structure where the Au atom occupies a noncentral site in a structure and the cluster has a less oblate shape. The corresponding eigenvalues, along with the associated orbitals, are shown in Fig. 7. The splitting between the filled d-states and the unoccupied D-state is only 1.14 eV, smaller than in the case of the $CuMg_8^-$ of 1.46 eV. The remaining D-orbitals also do not pair as in a square antiprism because the cluster has lower symmetry. Combined with earlier results on $ZnMg_8$, where the Zn atom occupies an exterior site, the progression in electronic structure from $ZnMg_8$ to $AuMg_8^-$ to $CuMg_8^-$ demonstrates how the D-shells in a spherical Jellium are modified as the cluster evolves toward a nonspherical shape, offering an alternate mechanism for stability. The interesting issue is that both oblate and spherical scenarios lead to a stable species, in one case via the splitting of the D-shell and in the other case via the close grouping of the D-states.

IV. CONCLUSIONS

To summarize, our studies show that the transition toward a NFE character in $ZnMg_n$ clusters proceeds more rapidly than in pure Mg_n clusters, with appreciable mixing of Mg p-states with Zn s-states. The electronic shell structure leads to stable $ZnMg_8$ and $ZnMg_9$ species, with a filled shell sequence of $1S^2\ 1P^6\ 1D^{10}$ for $ZnMg_8$. We further show that the D-supershell can be split by large amounts via oblate deformation. Such a splitting can stabilize clusters like $CuMg_8^-$ with an antiprism geometry, resulting in a subshell sequence $1S^2\ 1P^6\ 1D^8\ 2S^2$ separated from the split-off $1D_z^2$ state. Studies on $AuMg_8^-$ further indicate how the splitting can be reduced in oblate clusters with lower distortion. The prospect of clusters stabilized by shell splitting should encourage investigations into other systems with similar features. We are working with experimentalists to verify some of these findings by direct probing of electronic states through negative ion photo-detachment spectroscopy and velocity map imaging.

ACKNOWLEDGMENTS

The authors gratefully acknowledge support from the Air Force Office of Scientific Research (Grants No. FA9550-09-1-0371 and No. FA9550-10-1-0071). We acknowledge R. Flores-Moreno for his help in the implementation of the Gradient Embedded Genetic Algorithm - Guadalajara (GEGA-GDL) program in our calculations.

*snkhanna@vcu.edu

[1] A. W. Castleman Jr. and S. N. Khanna, J. Phys. Chem. C **113**, 2664 (2009).
[2] W. D. Knight, K. Clemenger, W. A. de Heer, W. A. Saunders, M. Y. Chou, and M. L. Cohen, Phys. Rev. Lett. **52**, 2141 (1984).
[3] W. A. de Heer, Rev. Mod. Phys. **65**, 611 (1993).
[4] S. N. Khanna and P. Jena, Phys. Rev. B **51**, 13705 (1995).
[5] D. E. Bergeron, P. J. Roach, A. W. Castleman Jr., N. O. Jones, and S. N. Khanna, Science **307**, 231 (2005).
[6] N. O. Jones, J. U. Reveles, S. N. Khanna, D. E. Bergeron, P. J. Roach, and A. W. Castleman Jr., J. Chem. Phys. **124**, 154311 (2006).
[7] P. J. Roach, A. C. Reber, W. H. Woodward, S. N. Khanna, and A. W. Castleman Jr., Proc. Natl. Acad. Sci. USA **104**, 14565 (2007).
[8] A. C. Reber, S. N. Khanna, P. J. Roach, W. H. Woodward, and A. W. Castleman Jr., J. Am. Chem. Soc. **129**, 169098 (2007).
[9] R. Burgert, H. Schnockel, A. Grubisic, X. Li, S. T. Stokes, K. H. Bowen, G. H. Gantefor, B. Kiran, and P. Jena, Science **319**, 438 (2008).
[10] P. J. Roach, W. H. Woodward, A. W. Castleman Jr., A. C. Reber, and S. N. Khanna, Science **323**, 492 (2009).
[11] S. A. Claridge, A. W. Castleman Jr., S. N. Khanna, C. B. Murray, A. Sen, and P. S. Weiss, ACS Nano **3**, 244 (2009).
[12] J. U. Reveles, P. A. Clayborne, A. C. Reber, S. N. Khanna, K. Pradhan, P. Sen, and M. R. Pederson, Nat. Chem. **1**, 310 (2009).
[13] P. J. Roach, W. H. Woodward, A. C. Reber, S. N. Khanna, and A. W. Castleman Jr., Phys. Rev. B **81**, 195404 (2010).
[14] J. U. Reveles, P. Sen, K. Pradhan, D. R. Roy, and S. N. Khanna, J. Phys. Chem. C **114**, 10739 (2010).
[15] M. Qian, A. C. Reber, A. Ugrinov, N. K. Chaki, S. Mandal, H. M. Saavedra, S. N. Khanna, A. Sen, and P. S. Weiss, ACS Nano **4**, 235 (2010).
[16] R. E. Leuchtner, A. C. Harms, and A. W. Castleman Jr., J. Chem. Phys. **91**, 2753 (1989).
[17] K. Clemenger, Phys. Rev. B **32**, 1359 (1985).
[18] E. Janssens, S. Neukermans, and P. Lievens, Curr. Opin. Sol. Matt. Sci. **8**, 185 (2004).
[19] S. N. Khanna, B. K. Rao, P. Jena, and J. L. Martins, in *Physics and Chemistry of Small Clusters*, edited by P. Jena, B. K. Rao, and S. N. Khanna, (Plenum Press, New York, 1987), p. 435.
[20] H.-P. Cheng, R. S. Berry, and R. L. Whetten, Phys. Rev. B **43** 10647 (1991).
[21] K. E. Schriver, J. L. Persson, E. C. Honea, and R. L. Whetten, Phys. Rev. Lett. **64**, 2539 (1990).
[22] T. Höltz, P. Lievens, T. Vezprémi, and M. T. Nguyen, J. Phys. Chem. C **113**, 21016 (2009).
[23] C. Bartels, C. Hock, J. Huwer, R. Kuhnen, J. Schwöbel, and B. von Issendorf, Science **323**, 1323 (2009).
[24] J. U. Reveles and S. N. Khanna, Phys. Rev. B **72**, 165413 (2005).
[25] M. Kosinen, P. Lipas, and M. Manninen, Z. Phys. D Atom. Mol. Cl. **35**, 285 (1995).

[26]J. Jellinek and P. H. Acioli, J. Phys. Chem. A **106**, 10919 (2002).
[27]deMon2k, A. M. Köster, P. Calaminici, M. E. Casida, R. Flores-Moreno, G. Geudtner, A. Goursot, T. Heine, A. Ipatov, F. Janetzko, J. M. del Campo, S. Patchkovskii, J. U. Reveles, D. R. Salahub, A. Vela, *deMon Developers* (Mexico, 2006), available at: [http://www.demon-software.com].
[28]J. P. Perdew, K. Burke, and M. Ernzerhof, Phys. Rev. Lett. **77**, 3865 (1996).
[29]P. Calaminici, F. Janetzko, A. Köster, R. Mejia-Olvera, and B. Zuniga-Gutierrez, J. Chem. Phys. **126**, 044108 (2007).
[30]P. Schwedtfeger, M. Dolg, W. H. E. Schwarz, G. A. Bowmaker, and P. D. W. Boyd, J. Chem. Phys. **91**, 1762 (1989).
[31]J. U. Reveles and A. M. Köster, J. Comput. Chem. **25**, 1109 (2004).
[32]R. Flores-Moreno, *GEGA-GDL* (Universidad de Guadalajara, Mexico, 2008–2010).
[33]W. J. Balfour and A. E. Douglas, Can. J. Phys. **48**, 901 (1970).
[34]N. W. Ashcroft and N. D. Mermin, *Solid State Physics*, international ed. (Saunders College Publishing, New York, 1976).
[35]S. F. Boys and F. Bernardi, Mol. Phys. **19**, 553 (1970).
[36]C. Kittel, *Introduction to Solid State Physics*, 7th ed. (John Wiley & Sons, New York, 1996).
[37]J. M. Merritt, V. E. Bondybey, and M. C. Heaven, Science **324**, 1548 (2009).
[38]S. N. Khanna, F. Reuse, and J. Buttet, Phys. Rev. Lett. **61**, 535 (1988).
[39]M. C. Heaven, J. M. Merritt, and V. E. Bondybey, Annu. Rev. Phys. Chem. **62**, 375 (2011).
[40]B. Kaiser and K. Rademann, Phys. Rev. Lett. **69**, 3204 (1992).
[41]A. Sanov and W. C. Lineberger, Phys. Chem. Chem. Phys. **6**, 2018 (2004).
[42]M. A. Sobhy, J. U. Reveles, U. Gupta, S. N. Khanna, and A. W. Castleman Jr., J. Chem. Phys. **130**, 054304 (2009).
[43]S. J. Peppernick, K. D. D. Gunaratne, and A. W. Castleman Jr., Proc. Natl. Acad. Sci. USA **107**, 975 (2010).